Preconditioning of the fluorescence diffuse optical tomography sensing matrix based on compressive sensing

An Jin,[1] Birsen Yazici,[1,2,*] Angelique Ale,[3] and Vasilis Ntziachristos[3]

[1]*Department of Biomedical Engineering, Rensselaer Polytechnic Institute, 110 Eighth Street, Troy, New York 12180, USA*

[2]*Department of Electrical, Computer, and Systems Engineering, Rensselaer Polytechnic Institute, 110 Eighth Street, Troy, New York 12180, USA*

[3]*Institute for Biological and Medical Imaging (IBMI), Helmholtz Zentrum München, Neuherberg D-85764, Germany*

**Corresponding author: yazici@ecse.rpi.edu*

Received July 20, 2012; revised August 30, 2012; accepted September 7, 2012; posted September 7, 2012 (Doc. ID 173053); published October 12, 2012

Image reconstruction in fluorescence diffuse optical tomography (FDOT) is a highly ill-posed inverse problem due to a large number of unknowns and limited measurements. In FDOT, the fluorophore distribution is often sparse in the imaging domain, since most fluorophores are designed to accumulate in relatively small regions. Compressive sensing theory has shown that sparse signals can be recovered exactly from only a small number of measurements when the forward sensing matrix is sufficiently incoherent. In this Letter, we present a method of preconditioning the FDOT forward matrix to reduce its coherence. The reconstruction results using real data obtained from a phantom experiment show visual and quantitative improvements due to preconditioning in conjunction with convex relaxation and greedy-type sparse signal recovery algorithms.

OCIS codes: 170.6960, 170.3880, 170.3010.

Fluorescence diffuse optical tomography (FDOT) is an imaging modality that uses near infrared light to measure 3D fluorophore activity inside biological tissue [1]. The FDOT inverse problem involves recovering the unknown fluorophore yield μ in a domain Ω from the measurements obtained on the domain boundary $\partial\Omega$ based on the following integral equation [1]:

$$\Gamma_{i,j} = \int_{\Omega} g_m^{(j)}(r)\phi_x^{(i)}(r)\mu(r), \tag{1}$$

where $\Gamma_{i,j}$ is the emission light field measured by the jth detector, $j = 1, \ldots, N_d$, due to the ith source, $i = 1, \ldots, N_s$, $\phi_x^{(i)}$ is the excitation field, $g_m^{(j)}$ is the Green's function of the diffusion equation, and N_s and N_d denote the number of sources and detectors, respectively.

Under the weak fluorophore assumption, we linearize (1) by assuming that the contribution of the fluorophore absorption to the total absorption is negligible. We discretize the imaging domain into N voxels, and organize all the measurements $\Gamma_{i,j}$ into a vector $\mathbf{\Gamma}$ of length $M = N_s \times N_d$. Taking into account the additive noise $\boldsymbol{\epsilon}$, the discretized form of (1) becomes

$$\boldsymbol{y} = \mathbf{\Gamma} + \boldsymbol{\epsilon} = \boldsymbol{A}\boldsymbol{x} + \boldsymbol{\epsilon}, \tag{2}$$

where $\boldsymbol{y}$ is the noisy measurement, $\boldsymbol{A}$ is the forward matrix, and $\boldsymbol{x}$ is the discretized fluorophore yield.

Most optical fluorophores are designed to accumulate in relatively small, specific regions in tissue, such as tumors. As a result, the fluorophore yield in the imaging domain is often very sparse. Compressive sensing (CS) theory shows that sparse signals can be recovered exactly from an underdetermined system when the underlying forward matrix is incoherent [2,3]. (See [4–6], for the recent applications of the sparse signal recovery techniques to optical tomography.) In many applications, a preconditioning matrix can be applied to the forward matrix to improve the recovery of sparse signals [2,3,7]. In [7], we decomposed the FDOT forward matrix into the Kronecker product of two underlying matrices: a matrix that depends on $\phi_x^{(i)}$, $i = 1, \ldots, N_s$ and another matrix that depends on $g_m^{(j)}$, $j = 1, \ldots N_d$. We designed two preconditioners to reduce the coherence of these two matrices, which, in turn, reduces the coherence of the FDOT forward matrix.

In this Letter, we use an alternative approach that directly preconditions the forward matrix $\boldsymbol{A}$. Let $\boldsymbol{M}_A$ be the preconditioning matrix. Then, (2) becomes

$$\boldsymbol{M}_A\boldsymbol{y} = \boldsymbol{M}_A\boldsymbol{A}\boldsymbol{x} + \boldsymbol{M}_A\boldsymbol{\epsilon} = \boldsymbol{A}_{\text{pre}} + \boldsymbol{M}_A\boldsymbol{\epsilon}, \tag{3}$$

where $\boldsymbol{A}_{\text{pre}}$ denotes the preconditioned forward matrix. To minimize the coherence of $\boldsymbol{A}_{\text{pre}}$, we seek to determine $\boldsymbol{M}_A$ such that the Gramm matrix $\boldsymbol{A}_{\text{pre}}^T\boldsymbol{A}_{\text{pre}}$ approximates the identity matrix. Let $\boldsymbol{U}_A\boldsymbol{\Sigma}_A\boldsymbol{V}_A^T$ be the singular value decomposition of $\boldsymbol{A}$. Following an approach similar to the one described in [3,7], the preconditioning matrix $\boldsymbol{M}_A$ is given by

$$\boldsymbol{M}_A = (\boldsymbol{\Sigma}_A\boldsymbol{\Sigma}_A^T)^{-1/2}\boldsymbol{U}_A^T. \tag{4}$$

In practice, $\boldsymbol{A}$ is usually ill-conditioned with a large number of singular values equal or close to 0. Therefore, $\boldsymbol{M}_A$ in (4) is also ill-conditioned. To mitigate this, we regularize (4) and write

$$\boldsymbol{M}_A = (\boldsymbol{\Sigma}_A\boldsymbol{\Sigma}_A^T + \lambda\boldsymbol{I})^{-1/2}\boldsymbol{U}_A^T, \tag{5}$$

where $\lambda \ll 1$ is a constant.

We next solve the following minimization problem to reconstruct the fluorophore yield

$$\min_{\boldsymbol{x}} \|\boldsymbol{x}\| \quad \text{such that} \quad \|\boldsymbol{y}_{pre} - \boldsymbol{A}_{pre}\boldsymbol{x}\|_2 \le \varepsilon, \tag{6}$$

0146-9592/12/204326-03$15.00/0

where $\|\boldsymbol{x}\|$ denotes either the ℓ_0- or ℓ_1-norm of $\boldsymbol{x}$. The optimization problem in (6) can be addressed by greedy-type or convex relaxation algorithms [2].

We evaluate the performance of FDOT image reconstruction due to the preconditioned forward matrix in conjunction with a variety of sparsity promoting algorithms using real data obtained in a phantom experiment. Figure 1(a) shows an illustration of the cylindrical phantom used in the experiment. The phantom was made of silicone rubber with about 2 cm in diameter, and 4 cm in length and had homogeneous absorption coefficient $\mu_a = 0.2\ \text{cm}^{-1}$ and scattering coefficient $\mu_s' = 12\ \text{cm}^{-1}$ $(D = 1/3(\mu_a + \mu_s'))$ at both the excitation and emission wavelengths (743 and 767 nm). It contained a hollow cylindrical tube in the middle with approximately 3 mm in diameter, which was filled with intralipid and ink to mimic the same optical properties as the background. The intralipid and ink contained 1 μM of Cy7 as the fluorophore. The cross section of the fluorophore yield at $z = 1$ cm is shown in Fig. 1(b).

The measurements were collected using the FDOT imaging system reported in [8]. Specifically, focused collimated laser beams were used as point light sources to excite the fluorophore. We had 60 point sources in total. The fluorescence measurements were collected by an electrically cooled CCD camera. The reading of the detector was recorded as the mean value of a subregion with 5×5 pixels around each detector location. We selected 60 detector locations. We discretized the imaging domain into $20 \times 20 \times 20$ voxels. Thus, the resulting forward sensing matrix was of dimension 3600 by 8000.

We evaluated the coherence of the forward matrix with and without the preconditioning matrix $\boldsymbol{M}_A$. The normalized inner product is a measure of the orthogonality (incoherence) of two different columns. It is defined as

$$r_{A_{p,q}} = \frac{|\langle \boldsymbol{a}_p, \boldsymbol{a}_q \rangle|}{\|\boldsymbol{a}_p\|_2 \|\boldsymbol{a}_q\|_2}, \tag{7}$$

where $\boldsymbol{a}_{p(q)}$ denotes the $p(q)$th column of $\boldsymbol{A}$. In general, the pth and qth columns are incoherent if $r_{A_{p,q}}$ has a small value. Figure 2 shows the normalized inner products between different pairs of columns arranged in a descending order. The largest 40% of the normalized inner products are presented, the rest 60% are close to 0, and thus omitted in the plot. Clearly, the application of $\boldsymbol{M}_A$ reduces the large correlations between different columns of $\boldsymbol{A}$. To quantify the improvement, we computed the relative area under the curves (AUC), which is given in the box in Fig. 2(a). We see that the preconditioning matrix reduces

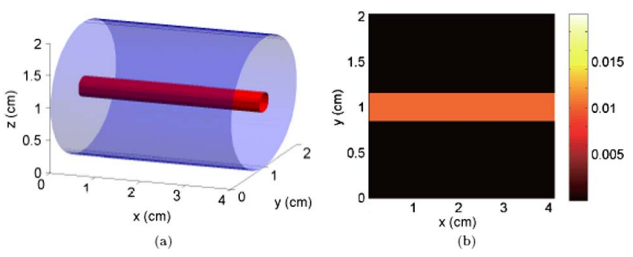

Fig. 1. (Color online) Configuration of (a) the silicon phantom and (b) the cross section of the fluorophore yield at $z = 1$ cm (middle) of the silicon phantom.

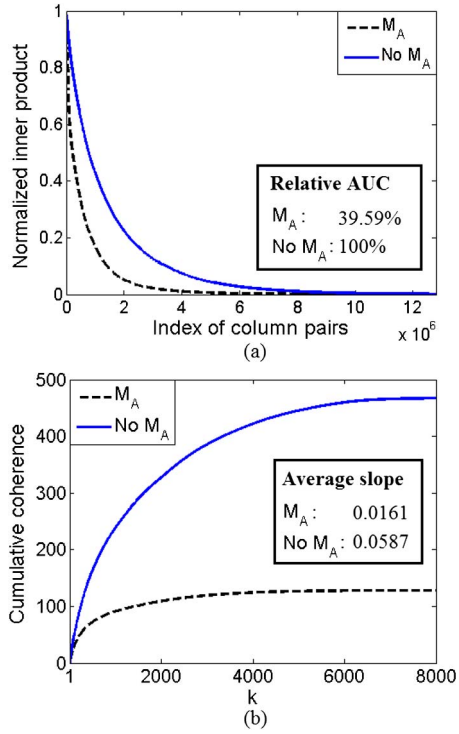

Fig. 2. (Color online) (a) Top 40% values of all the normalized inner products between different pairs of columns in $\boldsymbol{A}$ and (b) the cumulative coherence of $\boldsymbol{A}$ as a function of k.

$r_{A_{p,q}}$ $(1 \le p,\ q \le N)$, and the resultant AUC reduces to 39.59%. We also used cumulative coherence as a measure of the average coherence of $\boldsymbol{A}$. This quantity is defined as

$$\mathcal{M}_1(k, \boldsymbol{A}) = \max_{p} \max_{|Q|=k, p \notin Q} \sum_{q \in Q} \frac{|\langle \boldsymbol{a}_p, \boldsymbol{a}_q \rangle|}{\|\boldsymbol{a}_p\|_2 \|\boldsymbol{a}_q\|_2}, \tag{8}$$

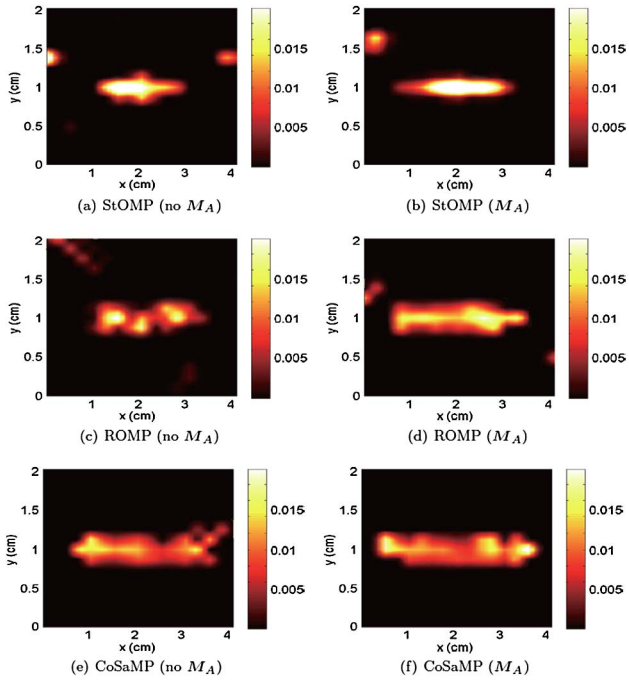

Fig. 3. (Color online) Cross sections at $z = 1$ cm (middle) of the reconstructed phantom using greedy algorithms.

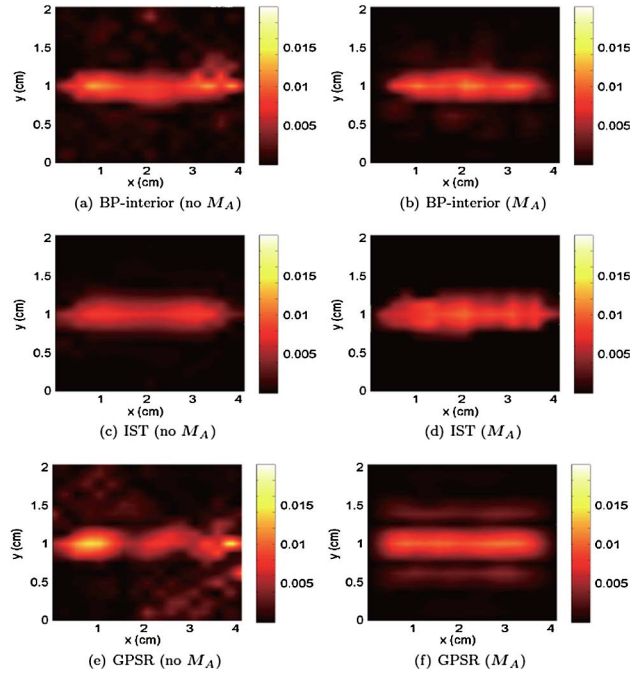

Fig. 4. (Color online) Cross sections at $z = 1$ cm (middle) of the phantom using convex relaxation techniques.

where Q is a subset of k columns in $\boldsymbol{A}$. $\mathcal{M}_1(k,\boldsymbol{A})$ is an monotonically nondecreasing function in k. If $\mathcal{M}_1(k,\boldsymbol{A})$ increase slowly, $\boldsymbol{A}$ is said to be quasi-incoherent [5]. Figure 2(b) shows the plot of the cumulative coherence. When $\boldsymbol{M}_A$ is applied, the cumulative coherence increases much slower. The average slope of each curve is provided in the box in Fig. 2(b).

To reconstruct the fluorophore yield, we used six different sparsity promoting reconstruction methods available in the CS literature [7]. Specifically, we used: stagewise orthogonal matching pursuit (StOMP), regularized orthogonal matching pursuit (ROMP), acrostic compressive sampling matching pursuit (CoSaMP), BP-interior, iterative shrinkage/thresholding (IST), and gradient projection for sparse reconstruction (GPSR). The first three are greedy-type algorithms, and the last three are convex relaxation based algorithms.

The cross sections of the reconstructed fluorophore yield maps using greedy-type algorithms are shown in Fig. 3, and those using convex relaxation techniques are shown in Fig. 4. We observe that the application of the preconditioning matrix results in reconstructed images that are in better agreement with the original fluorophore yield map. However, some background noise is also visible in the reconstructed images due to the large condition number of $\boldsymbol{M}_A$. The visual improvements are most obvious for the greedy-type algorithms. In simple greedy-type algorithms, the support of the signal is determined by selecting the columns of the forward matrix that have the greatest correlation with the measurements. The reduction of the coherence in the forward matrix has a direct effect on the column selection procedure at each iteration.

Table 1. SBNR of the Reconstructed Images Using Preconditioning and Different Sparsity Promoting Reconstruction Algorithms

Greedy	StOMP	ROMP	CoSaMP
$\boldsymbol{M}_A$	20.9	28.6	32.3
No $\boldsymbol{M}_A$	16.5	18.8	26.7
Relaxation	BP-interior	IST	GPSR
$\boldsymbol{M}_A$	23.8	19.8	22.1
No $\boldsymbol{M}_A$	14.9	17.1	12.3

To quantitatively assess the reconstruction results, we calculated the signal to background noise ratio (SBNR) of the reconstructed fluorophore yield map. SBNR is defined as the ratio between the mean value of the foreground fluorophore region and the standard deviation of the background. The results, summarized in Table 1, indicate the improvements in the image contrasts due to application of the preconditioning matrix using different sparse signal recovery algorithms.

In this Letter, we presented a method of preconditioning the FDOT forward matrix to reduce its coherence and demonstrated its performance in image reconstruction using real data. The results showed that the application of the preconditioning matrix reduces the coherence of the forward matrix and improves the visual and quantitative quality of the reconstructed images in conjunction with different sparse signal recovery algorithms. While we presented our approach for the linearized FDOT inverse problem, it can be easily extended to the nonlinear FDOT inverse problem within an iterative perturbation approach [9].

References

1. L. Zhou and B. Yazici, IEEE Trans. Image Process. **20**, 1094 (2011).
2. M. Elad, IEEE Trans. Signal Process. **55**, 5695 (2007).
3. J. Duarte-Carvajalino and G. Sapiro, IEEE Trans. Image Process. **18**, 1395 (2009).
4. P. Mohajerani, A. Eftekhar, J. Huang, and A. Adibi, Appl. Opt. **46**, 1679 (2007).
5. M. Suzen, A. Giannoula, and T. Durduran, Opt. Express **18**, 23676 (2010).
6. O. Lee, J. M. Kim, Y. Bresler, and J. C. Ye, IEEE Trans. Med. Imag. **15**, 13695 (2011).
7. A. Jin, B. Yazici, and V. Ntziachristos, "Light illumination and detection patterns for fluorescence diffuse optical tomography based on compressive sensing," IEEE Trans. Image Process. (to be published).
8. N. Deliolanis, T. Lasser, D. Hyde, A. Soubret, J. Ripoll, and V. Ntziachristos, Opt. Lett. **32**, 382 (2010).
9. S. Davis, H. Dehghani, J. Wang, S. Jiang, B. Pogue, and K. Paulsen, Opt. Express **15**, 4066 (2007).